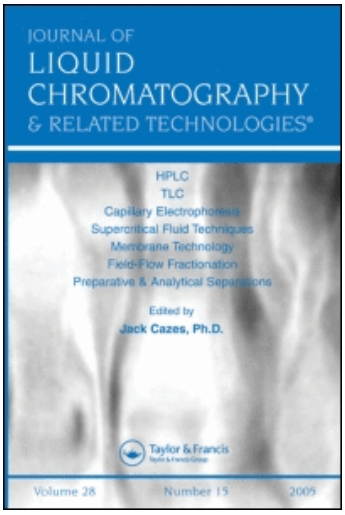

Journal of Liquid Chromatography & Related Technologies
Publication details, including instructions for authors and subscription information:
http://www.informaworld.com/smpp/title~content=t713597273

QUICK METHOD FOR THE DETERMINATION OF THE OPTIMAL OPERATING CONDITIONS OF A SIMULATED MOVING BED UNIT

Shih-Ming Lai[a]; Rong-Ren Loh[a]
[a] Department of Chemical Engineering, National Yunlin University of Science and Technology, Yunlin, Taiwan, Republic of China

Online publication date: 17 April 2002

To cite this Article Lai, Shih-Ming and Loh, Rong-Ren(2002) 'QUICK METHOD FOR THE DETERMINATION OF THE OPTIMAL OPERATING CONDITIONS OF A SIMULATED MOVING BED UNIT', Journal of Liquid Chromatography & Related Technologies, 25: 3, 345 — 361
To link to this Article: DOI: 10.1081/JLC-120008751
URL: http://dx.doi.org/10.1081/JLC-120008751

J. LIQ. CHROM. & REL. TECHNOL., 25(3), 345–361 (2002)

QUICK METHOD FOR THE DETERMINATION OF THE OPTIMAL OPERATING CONDITIONS OF A SIMULATED MOVING BED UNIT

Shih-Ming Lai* and Rong-Ren Loh

Department of Chemical Engineering, National Yunlin University of Science and Technology, 123, Sec. 3, University Road, Touliu, Yunlin, Taiwan, Republic of China

ABSTRACT

A four-column SMB laboratory unit for the continuous separation of enantiomers of 1-1′-bi-2-naphthol on Pirkle D-Phenylglycine was built, operated, and considered as a model system in this study. A quick and straightforward strategy presented determines the set of operating conditions that yield desired product purities for the SMB unit. This is based on the "triangle theory," and the good separation regions that take nonlinear equilibrium and mass-transfer effects into consideration were found based on the experimental results of a small number of SMB experiments. Good separation (purity and recovery of each isomer higher than 95%) was achieved for the model system. This method is shown to provide a convenient and reliable

*Corresponding author. E-mail: laism@yuntech.edu.tw

tool to find both optimal and robust operating conditions of SMB units.

INTRODUCTION

The simulated moving-bed (SMB) technology developed by UOP (1) has been used in the chemical industry for several bulk large-scale separations known as SORBEX processes. This technology has been recently applied in new areas, such as biotechnology, pharmaceuticals, and fine chemistry (2). Especially in the pharmaceutical industry, SMB is now considered to be the most promising technique for the preparative production of single enantiomeric drugs able to compete with current dominant techniques, such as elution batch chromatography, diastereoisomeric crystallization, and asymmetric synthesis (3).

The concept of the SMB is based in the true moving bed (TMB) process, where the liquid goes up and the solid goes down in each zone, and then countercurrent contact between solid and liquid occurs, leading to a high mass transfer driving force (Figure 1(a)). The liquid flowing out of section IV is recycled to section I, while the solid coming out of section I is recycled to section IV. The feed is continuously injected in the middle of the system and two product lines can be collected: the extract, rich in the more retained species, and the raffinate, rich in the less retained species. Unfortunately, the concept cannot really be implemented because of operating problems associated with the solid circulation in a TMB unit. This is the main reason why a SMB process is preferred. In the SMB technology (Figure 1(b)), the countercurrent movement is simulated by an appropriate flow switching sequence: the adsorbent bed is divided into a number of fixed-bed columns, while the inlet (eluent and feed) and outlet (extract and raffinate) lines move simultaneously, one column at fixed switch time intervals in the direction of the fluid phase flow.

The design of a SMB mainly relies on the appropriate choice of different operating parameters, i.e., liquid (recycle, feed, eluent, extract, raffinate) and solid (equivalent to the switch time) flow rates. Modeling and simulation of the SMB separation processes have gained increasing attention, because they could lead to significant saving in material and time, as the operating parameters could be determined during the technology development stage itself. There are two main strategies of modeling SMB processes: one is the real SMB model and the other is the equivalent TMB model. Although small differences will appear between these two strategies, the prediction of the performance of a SMB operation and proper selection of the above operating conditions can be done using the TMB approach (4).

The so-called "triangle theory," based on the TMB approach, provides explicit criteria for the choice of the proper operating conditions for both linear and non-linear systems (5–7); however, it has been developed under ideal conditions

(a)

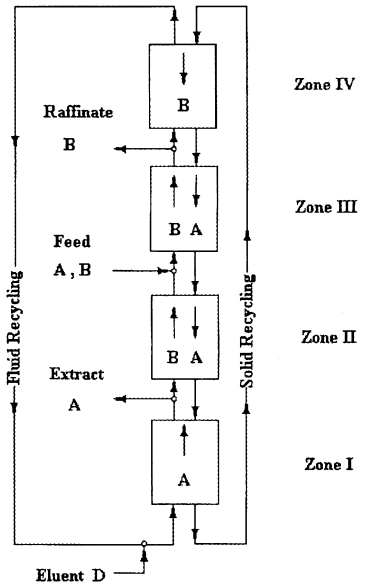

(b)

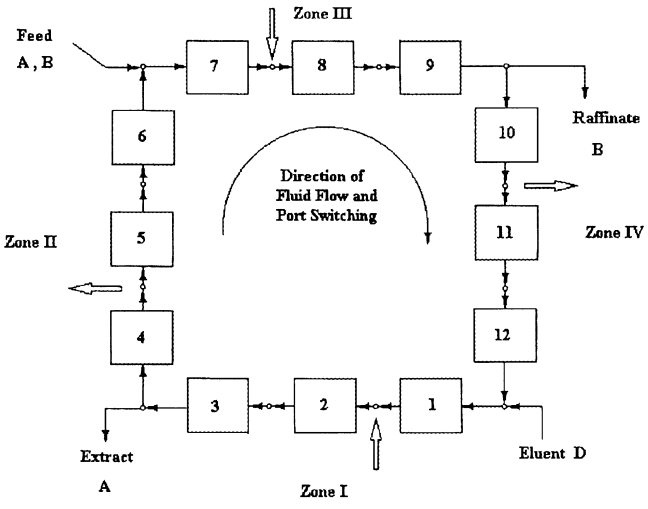

Figure 1. Sketch of the operating schemes. (a) Four-section TMB (b) Four-section SMB.

MARCEL DEKKER, INC.
270 Madison Avenue, New York, New York 10016

(axial dispersion and mass transfer resistance neglected). When mass-transfer effects are present, there is no explicit expression to define these limits. Azevedo and Rodrigues (8) solved, through simulation, the new limiting values for the flow-rate constraints in the presence of mass-transfer effects and showed that the complete separation region, proposed by the "triangle theory," is considerably reduced. Nevertheless, the reliability of their simulation has to be built on the accurate adsorption characteristics, including the equilibrium and kinetic model parameters.

The continuous separation of enantiomers of 1-1′-bi-2-naphthol in the chiral columns of Pirkle D-Phenylglycine using hexane-IPA (90:10) as eluent, by using the four-column SMB method, was considered as a model system in this study. The objective is to present a quick and straightforward strategy, without involving complicated mathematical models or tedious measurements of isotherm and kinetic parameters, for the optimal operation of the model system that takes non-linear equilibrium and mass-transfer effects into consideration. First, the "triangle theory" was used to provide guidelines for the selection of the feasible operating conditions. Then, the good separation regions in terms of operating conditions of the model system were found based on the experimental results of a small number of SMB experiments.

THEORETICAL BACKGROUND

Process Performance Parameters

The SMB performance is characterized by four process parameters: purity, recovery, solvent consumption, and adsorbent productivity. Table 1 defines the

Table 1. SMB Process Performance Parameters

Performance Parameters	Extract	Raffinate
Purity (%)	$\dfrac{\overline{C_{AE}}}{(\overline{C_{AE}}+\overline{C_{BE}})}$	$\dfrac{\overline{C_{BR}}}{(\overline{C_{BR}}+\overline{C_{AR}})}$
Recovery (%)	$\dfrac{Q_E\overline{C_{AE}}}{Q_F C_{AF}}$	$\dfrac{Q_R\overline{C_{BR}}}{Q_F C_{BF}}$
Solvent consumption (mL/mg)	$\dfrac{(Q_F+Q_D)}{Q_E\overline{C_{AE}}}$	$\dfrac{(Q_F+Q_D)}{Q_R\overline{C_{BR}}}$
Productivity (mg/min)	$Q_E\overline{C_{AE}}$	$Q_R\overline{C_{BR}}$

Where $\overline{C}$: time averaged concentration ($0 \sim t_s$), Q: flow rate.
Subscripts: A: more-retained species, B: less-retained species, E: extract, R: raffinate, F: feed, D: eluent.

process performance parameters for the case of a binary separation, in which the less retained species B is recovered in the raffinate, and the more retained species A is recovered in the extract.

Optimal Operation of a Simulated Moving-Bed

Due to the equivalence between SMB and TMB approaches, the operating conditions of a SMB separator can be optimized using the TMB approach (4). The design problem of a TMB consists on setting the proper operating conditions (liquid and solid flow rates) to obtain the desired separation. In order that the less retained species moves in the direction of the liquid phase and the more retained one in the direction of the solid phase, some constraints have to be satisfied in each column. The constraints, defining a complete separation in a TMB unit for a linear equilibrium binary system in the absence of dispersion and mass-transfer effects, can be expressed as (9,10):

$$\begin{aligned} &\frac{Q_{\mathrm{I}}C_{\mathrm{AI}}}{Q_{\mathrm{S}}q_{\mathrm{AI}}} > 1; \quad \frac{Q_{\mathrm{II}}C_{\mathrm{BII}}}{Q_{\mathrm{S}}q_{\mathrm{BII}}} > 1 \text{ and } \frac{Q_{\mathrm{II}}C_{\mathrm{AII}}}{Q_{\mathrm{S}}q_{\mathrm{AII}}} < 1; \\ &\frac{Q_{\mathrm{III}}C_{\mathrm{BIII}}}{Q_{\mathrm{S}}q_{\mathrm{BIII}}} > 1 \text{ and } \frac{Q_{\mathrm{III}}C_{\mathrm{AIII}}}{Q_{\mathrm{S}}q_{\mathrm{AIII}}} < 1; \quad \frac{Q_{\mathrm{IV}}C_{\mathrm{BIV}}}{Q_{\mathrm{S}}q_{\mathrm{BIV}}} < 1 \end{aligned} \tag{1}$$

where C_{ij} and q_{ij} are the fluid-phase and average-absorbed-phase concentrations of species i ($i = $ A, B) in the section j ($j = $ I, II, III, IV), respectively, Q_j is the internal liquid flow rate in the section j.

The same constraints can be expressed alternatively in terms of fluid and solid velocities. Defining the parameter γ_j as the ratio between fluid and solid velocities, i.e., $\gamma_j = v_j/u_{\mathrm{s}}$, the constraints defined by Equation (1) becomes:

$$\begin{aligned} &\gamma_{\mathrm{I}} > FK_{\mathrm{A}}; \quad FK_{\mathrm{B}} < \gamma_{\mathrm{II}} < FK_{\mathrm{A}}; \\ &FK_{\mathrm{B}} < \gamma_{\mathrm{III}} < FK_{\mathrm{A}}; \quad \gamma_{\mathrm{IV}} < FK_{\mathrm{B}} \end{aligned} \tag{2}$$

where $K_i = q_{ij}/C_{ij}$ is the Henry's constant of species i in the section j, ε is the total column porosity, v_j is the interstitial fluid velocity, u_{s} is the equivalent interstitial solid velocity in the TMB process, and $F = (1 - \varepsilon)/\varepsilon$ is the phase ratio. These constraints are in accordance with the equilibrium model results first proposed by Storti et al. (11). In a $\gamma_{\mathrm{II}} \times \gamma_{\mathrm{III}}$ plane, this region corresponds to the square triangle shown in Figure 2. Inside this square triangle, any (γ_{II}, γ_{III}) pair yields complete separation provided the constraints on γ_{I} and γ_{IV} are not violated.

The liquid flow rates in a TMB process include the four internal liquid flow rates: $Q_{\mathrm{I}}, Q_{\mathrm{II}}, Q_{\mathrm{III}}, Q_{\mathrm{IV}}$ (or Q_{recycle}) and the four external flow rates: $Q_{\mathrm{F}}, Q_{\mathrm{D}}, Q_{\mathrm{E}}, Q_{\mathrm{R}}$, which are related by the overall mass balances at the nodes of the four sections. Therefore, there are only four independent variables among them and Q_{F}, Q_{D}, Q_{E} (or Q_{R}) and Q_{recycle} are usually set in the process. The four

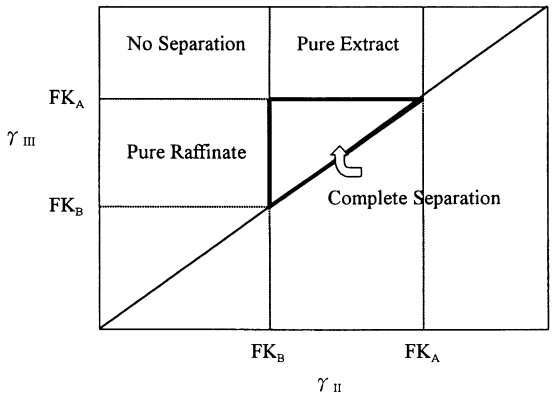

Figure 2. The complete separation region in a $\gamma_{II} \times \gamma_{III}$ plane.

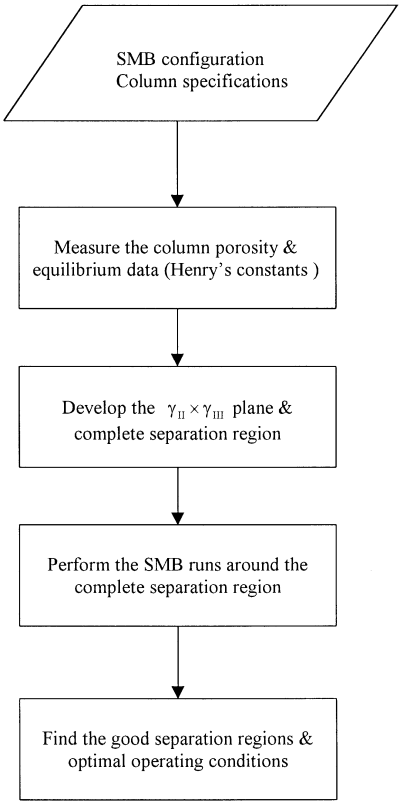

Figure 3. General procedure for the optimal operation of a SMB unit.

MARCEL DEKKER, INC.
270 Madison Avenue, New York, New York 10016

liquid flow rates, together with the solid flow rate (Q_s), have to be properly chosen based on the constraints of Equation (2). Finally, since both SMB and TMB systems have similar cyclic steady-state performances, the estimation of TMB operating conditions can be applied for the SMB. The switch time t_s in SMB operation can be calculated from the solid velocity of TMB by: $u_s = L_c/t_s$, where L_c is the length of the column. The liquid velocities or flow rates v_j^* or Q_j^* of SMB in four sections are evaluated by: or $v_j^* = v_j + u_s$ or $Q_j^* = Q_j + Q_s/F$.

The strategy used to find the region of good separation, accounting for the effects of non-linear equilibrium, axial dispersion, and mass-transfer resistance, is described in Figure 3. First, a TMB flow rate optimization strategy, proposed by the "triangle theory" considering linear and ideal conditions as explained above, was used to develop a complete separation region. The only parameters needed to be provided are the equilibrium Henry's constants of each isomer, which were measured by the elution chromatographic method (12–14). Then, the four-column SMB experiments were run with the operating conditions selected around the complete separation region. Finally, the optimal operating conditions and separation performances were found based on the experimental results.

EXPERIMENTAL

The model system to be studied in this work is the separation of 1-1′-bi-2-naphthol enantiomers using Pirkle covalent D-phenylglycine (3,5-dinitrobenzoyl derivative of phenylglycine covalently bonded to aminopropyl silica gel) as chiral stationary phase and mobile phase composition of 90/10 (vol/vol) hexane/isopropanol (IPA) as the eluent.

Columns and Chemicals

One analytical column of 25.0 cm L × 0.46 cm ID and 5 μm particle diameter and four semi-preparative columns of 10.0 cm L × 1.0 cm ID and 10 μm particle diameter purchased from Regis (Morton Grove, IL, USA) were used in this study. (R)-(+)-1-1′-bi-2-naphthol (R-form, 99% pure, formula weight 286.33), (S)-(−)-1-1′-bi-2-naphthol (S-form, 99% pure, formula weight 286.33), and 1,3,5-tri-tert-butyl benzene (TTBB, 99%, formula weight 246.44) were purchased from Aldrich (Milwaukee, WI, USA). HPLC grade hexane and IPA were purchased from Tedia (Fairfield, OH, USA).

Analytical Chromatographic System

A high performance liquid chromatograph (HPLC) system includes a Jasco Model PU-980 solvent metering pump, a Jasco Model UV-970 UV detector

MARCEL DEKKER, INC.
270 Madison Avenue, New York, New York 10016

(Tokyo, Japan), a Rheodyne Model 7125 6-way syringe loading valve fitted with a 20-μL sample loop (Cotati, CA, USA), and a Sunway Model 940-CO column oven (Taipei, Taiwan). The millivolt signal from the detector was converted to digital form with the aid of an analog-to-digital interface card (Scientific Information Service Corp., Taiwan) interfaced with a microcomputer for data storage and processing.

The adsorption characteristics and bed porosity of each of the four semi-preparative columns (10.0 cm L × 1.0 cm ID and 10 μm) used were measured by the elution chromatographic method (12–14) using the above HPLC system.

SMB Laboratory Unit

The SMB system is a laboratory scale continuous chromatography system as described in Figure 4. It consists of four semi-preparative columns (10.0 cm L × 1.0 cm ID and 10 μm) arranged in a 1-1-1-1 configuration, i.e., one column per section. The fluid stream coming out of the fourth section is collected in a storage flask and recycled to section I, which forms the closed-loop configuration. The four columns are located in a water bath, where the temperature is controlled at 30°C.

With reference to Figure 4, five flows (feed, eluent, extract, raffinate, and recycled eluent) have to be handled in the unit. The two inlet streams (feed

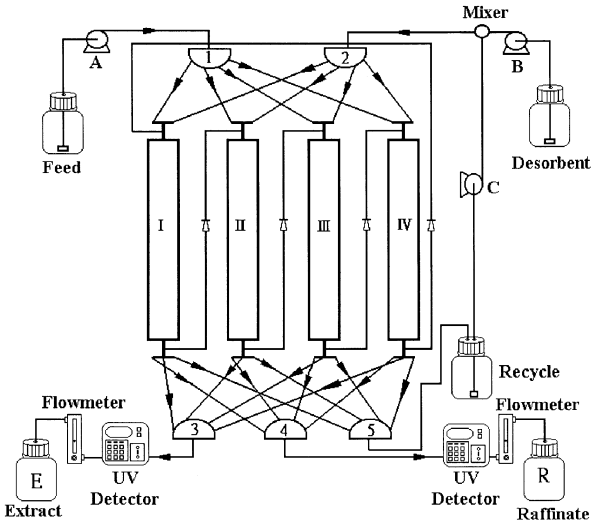

Figure 4. Scheme of the four-column SMB laboratory-unit. Half-circles: 1. Feed valve, 2. Solvent valve, 3. Extract valve, 4. Raffinate valve, 5. Recycle valve; Pumps: A. Feed pump, B. Solvent pump, C. Recycle pump.

and eluent) are controlled by two MPLC pumps (SSI Series III, USA). The two outlet streams (extract and raffinate) are controlled by two flow meters (AALBORG, NY, USA). The flow rate of the fluid stream coming out of the fourth section is determined by the overall mass balance of the SMB unit, and the recycled eluent coming out of the storage flask is controlled by one MPLC pump (SSI Series III).

Five electropneumatic 12-port multiposition valves (VICI-Valco EMTCSD12UW, Schenkon, Switzerland) are controlled by a computer to actuate the SMB. One valve is connected to the feed port, one to the solvent port, one to the raffinate port, one to the extract port, and the last one to the recycle port. The movement of each valve is controlled by V-PD-MICROEA software (VICI-Valco). The T joints at the top and bottom of each column allow them to be connected in series or to a recycling line. To avoid back mixing, four check valves are placed on the lines connecting each column to the following one.

All the lines in the unit are made of stainless steel and have 0.50 mm ID. Although the unit only consists of four columns, a set up with more columns (up to 12 columns) can be easily done with slight modification of the tubing connections.

Two ISCO Retriever 500 fraction collectors (Lincoln, NE, USA) were used to collect the samples of the two outlet streams, i.e., extract and raffinate, for each cycle. The concentration and purity of each sample were analyzed on the analytical chiral column (25.0 cm L × 0.46 cm ID and 5 μm) using the standard analytical chromatographic system described above. The absorbance wavelength was set at 254 nm. Meanwhile, two UV spectrophotometric detectors (Jasco UV-970 with a preparative cell), all operating at 347 nm, were connected to the SMB unit as shown in Figure 4. They were located on the extract line, between the extract position valve and the extract flow meter, and on the raffinate line, between the raffinate position valve and the raffinate flow meter, respectively. They monitor the concentration histories at these two ports.

RESULTS AND DISCUSSION

Determination of the Adsorption Characteristics and Bed Porosity

The adsorption characteristics, including the retention factor (or Henry's constant) of each of the isomers (K_R and K_S), the separation factor (α), and the column efficiency (or number of theoretical plates) of each of the isomers (N_R and N_S), of the four semi-preparative columns used were measured for both isomers. Also, the total bed porosity (ε) was determined using TTBB, which is nonadsorbable on the chiral column. The results are listed in Table 2. The relative standard deviations (RSD) of the column efficiencies of the two components are larger, which means the column efficiency is much less reproducible than the other column parameters. The low average value of the separation factor,

Table 2. Adsorption Characteristics of the Semi-preparative Columns Used

Column	ε	F	K_R	K_S	α	N_R	N_S
A	0.726	0.378	4.250	3.435	1.237	3923	3861
B	0.729	0.371	4.332	3.618	1.197	3601	3696
C	0.725	0.380	4.304	3.403	1.265	3907	3937
D	0.728	0.373	4.292	3.542	1.212	3913	3907
Average	0.727	0.376	4.295	3.500	1.228	3836	3850
Std	0.002	0.004	0.034	0.100	0.030	157	107
RSD%	0.248	1.117	0.794	2.826	2.427	4.088	2.792

Flow rate: 4.0 mL/min.

$\alpha = 1.25 \sim 1.30$, suggests that the separation of the two components is a difficult one to perform with the SMB unit.

Arrangement of the Experimental Runs

Using the average values of the total bed porosity and retention factors of Table 2, the square triangle region of complete separation in the $\gamma_{II} \times \gamma_{III}$ plane, formed by the flow constraints proposed by the linear and ideal model, was plotted as shown in Figure 5. The complete separation region was then referred to select the proper operating conditions of the SMB unit. Table 3 shows the two

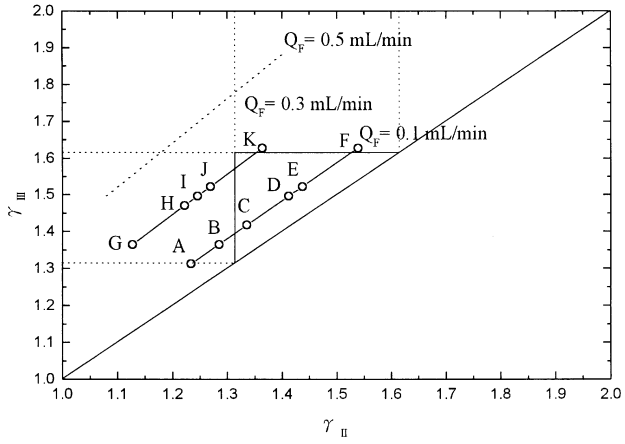

Figure 5. Location of the operating points of the experimental runs in the $\gamma_{II} \times \gamma_{III}$ plane ($Q_F + Q_D = 2.5$ mL/min).

Table 3. Operation Conditions of the Experimental Runs ($C_F = 2.290$ mg/mL; $Q_F + Q_D = 2.5$ mL/min)

Set No.	Run No.	Q_F mL/min	Q_D mL/min	Q_E mL/min	Q_R mL/min	$Q_{recycle}$ mL/min	t_s min	γ_I	γ_{II}	γ_{III}	γ_{IV}
1	A	0.1	2.4	1.1	1.4	1.6	4.4	2.0824	1.2347	1.3118	0.2330
	B	0.1	2.4	1.1	1.4	1.6	4.5	2.1525	1.2855	1.3643	0.2610
	C	0.1	2.4	1.1	1.4	1.6	4.6	2.2225	1.3363	1.4169	0.2890
	D	0.1	2.4	1.1	1.4	1.6	4.75	2.3276	1.4125	1.4957	0.3310
	E	0.1	2.4	1.1	1.4	1.6	4.8	2.3626	1.4379	1.5220	0.3450
	F	0.1	2.4	1.1	1.4	1.6	5.0	2.5027	1.5395	1.6270	0.4011
2	G	0.3	2.2	1.1	1.4	1.6	4.5	1.9948	1.1279	1.3643	0.2610
	H	0.3	2.2	1.1	1.4	1.6	4.7	2.1279	1.2225	1.4694	0.3170
	I	0.3	2.2	1.1	1.4	1.6	4.75	2.1612	1.2461	1.4957	0.3310
	J	0.3	2.2	1.1	1.4	1.6	4.8	2.1945	1.2698	1.5220	0.3451
	K	0.3	2.2	1.1	1.4	1.6	5.0	2.3276	1.3643	1.6270	0.4011

Constraints for γ_I and γ_{IV}: $\gamma_I > FK_R = 1.6147$; $\gamma_{IV} < FK_S = 1.3143$.

MARCEL DEKKER, INC.
270 Madison Avenue, New York, New York 10016

sets of experimental runs performed with operating conditions in terms of liquid flow rates, Q_F, Q_D, Q_E, Q_R and $Q_{recycle}$, switch time, t_s, and generalized flow rate ratios, γ_j; j=I, II, III, IV. The feed concentration of the racemic mixture was fixed at 2.29 mg/mL, which is lower than its solubility limit of 3.72 mg/mL (15). The Q_E, Q_R, and $Q_{recycle}$ values and sum of flow rates of inlet/outlet streams, i.e., $Q_F + Q_D = Q_E + Q_R$ value ($= 2.5$ mL/min), were fixed for all runs in the two sets, whereas the Q_F and Q_D values were varied from set to set. It is worth noting that all the constraints on γ_I and γ_{IV} of each experiment are not violated, as shown in Table 3.

Figure 5 also shows the location of the operating points of experiments in the $\gamma_{II} \times \gamma_{III}$ plane, which is compared to that of the complete separation region. As can be seen in Table 3, the liquid flow rates in each of the two sets of experiments have been kept constant, whereas the switch time has been changed. This creates a straight line in the $\gamma_{II} \times \gamma_{III}$ plane nearly parallel to the diagonal and across the complete separation region, as shown in Figure 5.

SMB System Performance

Table 4 shows the experimental results in terms of steady state concentrations, optical purities, recoveries, product productivities, and solvent consumptions of the extract and raffinate streams. Figures 6(a) and 6(b) show the histories of the extract and raffinate concentrations and Figures 7(a) and 7(b) show the histories of the averaged extract and raffinate purities of run D, respectively. It can be observed that the system takes about 8 cycles (about 2.5 hours) to reach the periodic-steady state. The SMB was run for 15 cycles.

The first set, i.e., runs A–F, corresponds to operating points belonging to the straight line closer to the diagonal line in Figure 5. By increasing the switch time from 4.4 to 5.0 min, the experimental purity values, as a function of the switch time, exhibit the expected pattern of behavior, i.e., the raffinate purity decreases steadily while the extract purity increases from run A to run F. The best overall separation performance is achieved in run D, where the raffinate purity of 100% and the extract purity of 97% were obtained. The system performance, as a function of the switch time of the second set of experiments, exhibits the same pattern of behavior as the first set. The best overall separation performance obtained for the second set is the raffinate purity of 100% and the extract purity of 90% in run I. Since the feed flow rate in the second set is higher than the first set, the second set has the higher productivity.

The differences in the system performances between the two sets are as follows. First, the larger the feed flow rate, the larger the productivity, but the lower the feed rate, the better will be the separation performance achieved, i.e. the product purity can be improved by reducing the feed flow rate; however,

Table 4. Separation Performance of the Four-Column SMB System

Run No.	Q_F mL/min	C_F mg/mL	t_s min	$P_{E(A)}$ %	$P_{R(B)}$ %	$C_{E(A)}$ mg/mL	$C_{E(B)}$ mg/mL	$C_{R(A)}$ mg/mL	$C_{R(B)}$ mg/mL	$REC_{E(A)}$ %	$REC_{R(B)}$ %	$SOL_{E(A)}$ mL/mg	$SOL_{R(B)}$ mL/mg	$PRO_{E(A)}$ mg/min	$PRO_{R(B)}$ mg/min
A	0.1	2.290	4.4	82	100	0.104	0.023	0	0.064	100	78	21.83	27.98	0.115	0.089
B	0.1	2.290	4.5	95	100	0.104	0.005	0	0.077	100	95	21.83	23.05	0.114	0.108
C	0.1	2.290	4.6	96	100	0.104	0.004	0	0.078	100	96	21.83	22.78	0.115	0.110
D	0.1	2.290	4.75	97	100	0.104	0.003	0	0.079	100	97	21.83	22.53	0.115	0.110
E	0.1	2.290	4.8	97	91	0.094	0.003	0.008	0.079	90	97	24.16	22.46	0.103	0.111
F	0.1	2.290	5.0	94	71	0.063	0.004	0.032	0.079	61	96	35.95	22.72	0.070	0.110
G	0.3	2.292	4.5	70	100	0.313	0.134	0	0.140	100	57	7.27	12.73	0.344	0.196
H	0.3	2.292	4.7	88	100	0.312	0.043	0	0.212	100	86	7.28	8.43	0.344	0.297
I	0.3	2.292	4.75	90	100	0.313	0.035	0	0.218	100	89	7.27	8.18	0.344	0.306
J	0.3	2.292	4.8	97	88	0.271	0.008	0.033	0.239	87	97	8.39	7.48	0.298	0.334
K	0.3	2.292	5.0	97	66	0.154	0.005	0.125	0.242	49	98	14.76	7.38	0.169	0.339

P: product purity, REC: recovery, SOL: solvent consumption, PRO: productivity.
Subscripts: (A): R-isomer, (B): S-isomer, E: extract, R: raffinate, F: feed.

MARCEL DEKKER, INC.
270 Madison Avenue, New York, New York 10016

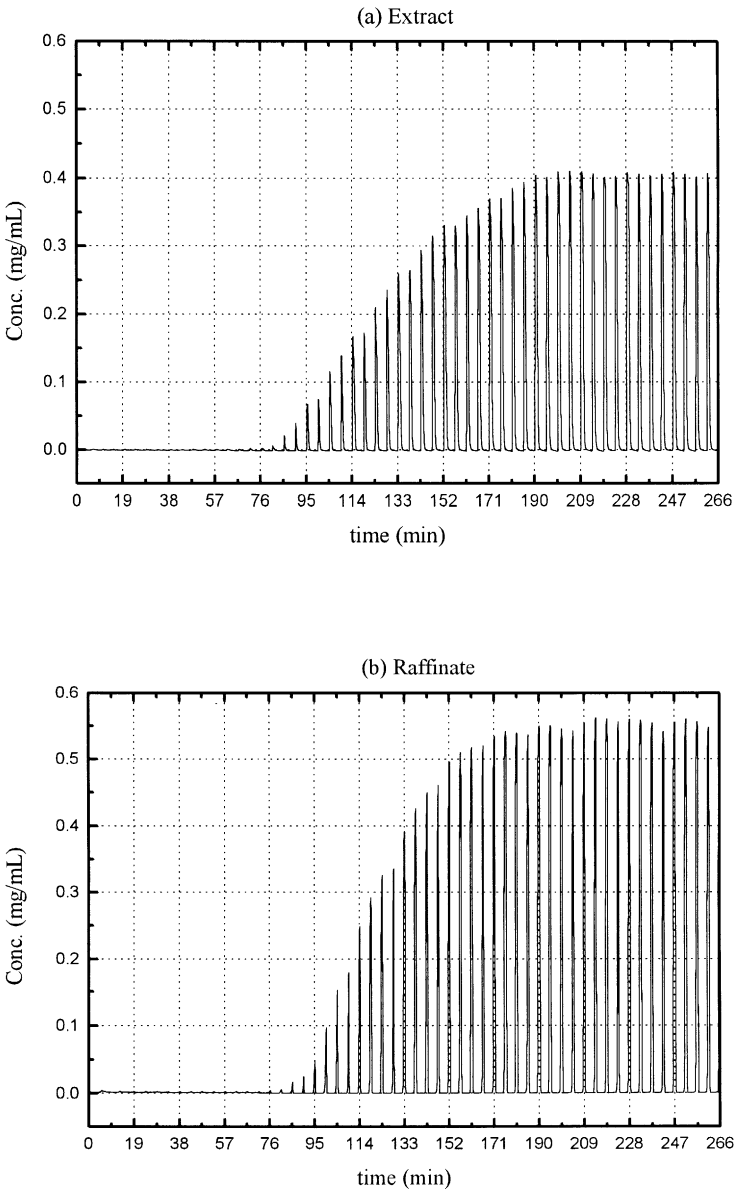

Figure 6. The histories of the extract and raffinate concentrations of run D.

MARCEL DEKKER, INC.
270 Madison Avenue, New York, New York 10016

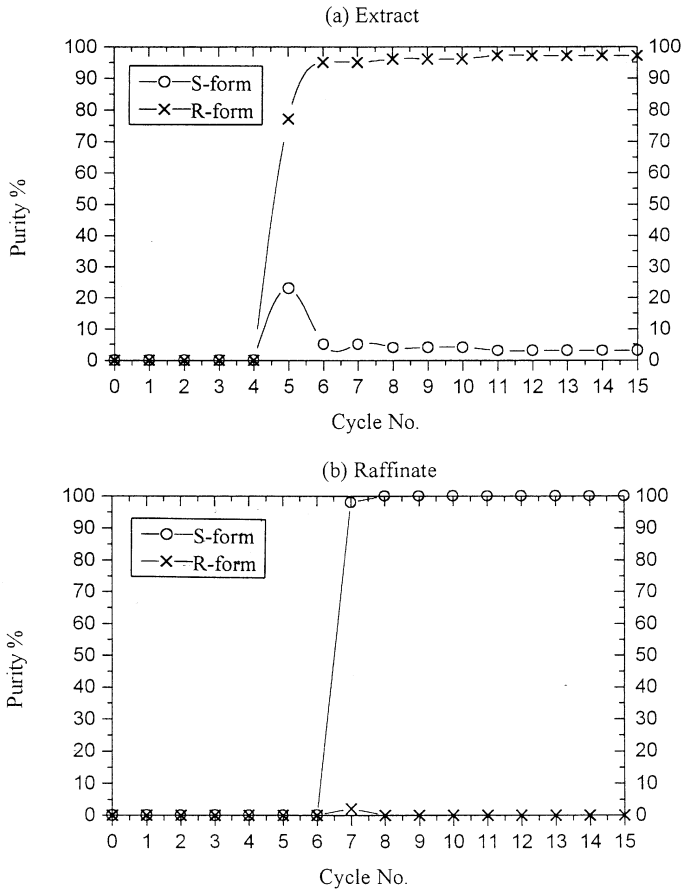

Figure 7. The histories of the averaged purities in each cycle of Run D.

the product productivity is also reduced. There must be a compromise between these two performances. Secondly, the range of operating conditions achieving the best product purity of each set becomes smaller when increasing the feed flow rate, i.e., the separation conditions become less robust, which means the proper selection of the switch time is very important.

Determination of the Region of Good Separation

Based on the above experimental results (Table 4), the separation regions on the $\gamma_{II} \times \gamma_{III}$ plane having different purity requirements (90%, 95% and 98%) were

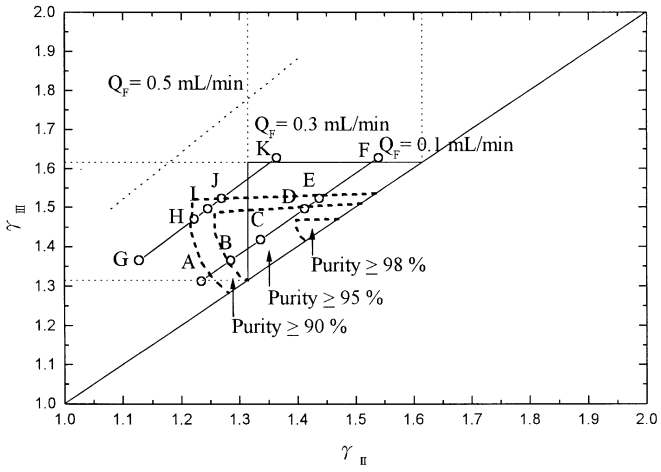

Figure 8. The predicted good separation regions ($C_F = 2.290\,mg/mL$; $Q_F + Q_D = 2.5\,mL/min$).

predicted, as shown in Figure 8. The two-point boundary was determined by the desired purity, in which every operating condition inside the boundary possessed product purity higher than the desired purity. The distance between the boundary points reduced and finally disappeared with increasing feed flow rate. Connecting all the boundary points formed the separation region of the desired product purity. The same process was repeated for the different desired product purity.

From the location of the good separation regions in Figure 8, the corresponding operating conditions to obtain a certain system performance can be determined. Comparison with the complete separation region indicates that the separation triangle is twisted leftward and downward and is significantly reduced. The deformation is due to the non-linear equilibrium, as simulated by Mazzotti et al. (5) Gentilini et al. (6) and Migliorini et al. (7) while the reduction is due to the non-ideal conditions, as simulated by Azevedo and Rodrigues (8).

CONCLUSIONS

This study provides a quick and straightforward strategy for the optimal operation of a SMB unit without involving complicated mathematical models or tedious measurements of isotherm and kinetic parameters. The good separation regions, in terms of operating conditions of the real system that accounts for the non-linear equilibrium and mass-transfer effects, were found based on the experimental results of a small number of SMB experiments, which were selected around the complete separation region, proposed by the "triangle theory."

For our model system, the continuous separation of 1,1′-bi-2-naphthol enantiomers in the Pirkle D-Phenylglycine chiral columns, carried out in a four-bed SMB unit, with good separation (purities and recoveries higher than 95% in the extract and raffinate) was obtained for the case of low feed flow rate (0.1 mL/min). By increasing the feed flow rate, productivity was improved at the expense of purity and robustness of the operation. When the feed flow rate was increased to 0.3 mL/min, purities and recoveries in the extract and raffinate were reduced to only 90%. The product purity and robustness of the operation deteriorated dramatically as the feed flow rate was further increased. The system performances, in terms of product purity and productivity can be both improved by either increasing the column length of the four-bed SMB unit, or running the more bed (eight-bed or twelve-bed) SMB unit. Work along these directions is currently in progress.

ACKNOWLEDGMENT

The authors wish to thank the National Science Council of the Republic of China for the financial support under grant no. NSC 88-2214-E-224-001 and NSC 89-2214-E-224-007.

REFERENCES

1. Broughton, D. B.; Gerhold, C. G. U.S. Patent No. 2,985,589, 1961.
2. Nicoud, R. M. LC-GC Int. **1992**, *5* (5), 43.
3. Stinson, S. C. Chem. Eng. News **1955**, 44.
4. Pais, L. S.; Loureiro, J. M.; Rodrigues, A. E. AIChE. J. **1998**, *44* (3), 561.
5. Mazzotti, M.; Storti, G.; Morbidelli, M. J. Chromatogr. **1997**, *769*, 3.
6. Gentilini, A.; Migliorini, C.; Mazzotti, M.; Morbidelli, M. J. Chromatogr. **1998**, *805*, 37.
7. Migliorini, C.; Mazzotti, M.; Morbidelli, M. J. Chromatogr. **1998**, *827*, 161.
8. Azevedo, C. S.; Rodrigues, A. E. AIChE. J. **1999**, *45* (5), 956.
9. Ruthven, D. M.; Ching, C. B. Chem. Eng. Sci. **1989**, *44*, 1011.
10. Zhong, C.; Guiochon, G. Chem. Eng. Sci. **1996**, *51*, 4307.
11. Storti, G.; Mazotti, M.; Morbidelli, M.; Carra, S. AIChE. J. **1993**, *39*, 471.
12. Miyabe, K.; Suzuki, M. AIChE. J. **1992**, *38*, 6.
13. Lim, B. -G.; Ching, C. B. Ind. Eng. Chem. Res. **1996**, *35.*
14. Lai, S. M.; Lin, Z. C. Sep. Sci. & Tech. **1999**, *34* (16), 3173.
15. Lai, S. M.; Lin, Z. C.; Loh, R. R. J. Chin. Inst. Chem. Engrs. **2000**, *31* (5), 507.

Received August 20, 2001
Accepted September 15, 2001
Manuscript 5640

Request Permission or Order Reprints Instantly!